

Label-free quality control and identification of human keratinocyte stem cells by deep learning-based automated cell tracking

Takuya Hirose¹ | Jun'ichi Kotoku¹ | Fujio Toki² | Emi K. Nishimura^{2,3} | Daisuke Nanba² 

¹Graduate School of Medical Care and Technology, Teikyo University, Tokyo, Japan

²Department of Stem Cell Biology, Medical Research Institute, Tokyo Medical and Dental University (TMDU), Tokyo, Japan

³Division of Aging and Regeneration, Institute of Medical Science, The University of Tokyo, Tokyo, Japan

Correspondence

Jun'ichi Kotoku, PhD, Graduate School of Medical Care and Technology, Teikyo University, 2-11-1 Kaga, Itabashi-ku, Tokyo 173-8605, Japan.

Email: kotoku@med.teikyo-u.ac.jp

Daisuke Nanba, PhD, Department of Stem Cell Biology, Medical Research Institute, Tokyo Medical and Dental University (TMDU), 1-5-45 Yushima, Bunkyo-ku, Tokyo 113-8510, Japan.

Email: nanbscm@tmd.ac.jp

Funding information

Grand-in-Aid for Scientific Research on Innovative Area "Singularity Biology (No.8007)" of The Ministry of Education, Culture, Sports, Science, and Technology, Japan, Grant/Award Number: 19H05418; Japan Society for the Promotion of Science, Grant/Award Number: 17K102319; Okawa Foundation for Information and Telecommunications, Grant/Award Number: 19-08

Abstract

Stem cell-based products have clinical and industrial applications. Thus, there is a need to develop quality control methods to standardize stem cell manufacturing. Here, we report a deep learning-based automated cell tracking (DeepACT) technology for noninvasive quality control and identification of cultured human stem cells. The combination of deep learning-based cascading cell detection and Kalman filter algorithm-based tracking successfully tracked the individual cells within the densely packed human epidermal keratinocyte colonies in the phase-contrast images of the culture. DeepACT rapidly analyzed the motion of individual keratinocytes, which enabled the quantitative evaluation of keratinocyte dynamics in response to changes in culture conditions. Furthermore, DeepACT can distinguish keratinocyte stem cell colonies from non-stem cell-derived colonies by analyzing the spatial and velocity information of cells. This system can be widely applied to stem cell cultures used in regenerative medicine and provides a platform for developing reliable and noninvasive quality control technology.

KEYWORDS

cell motion analysis, deep learning, keratinocyte stem cells, quality control, stem cell cultures

1 | INTRODUCTION

Stem cells, including pluripotent and tissue-specific stem cells have various clinical applications.¹ The quality of the cultured stem cells is crucial

for successful application in regenerative medicine. Hence, these stem cells must be maintained and expanded *ex vivo* under carefully controlled conditions. However, the quality control of stem cell cultures is currently based on visual inspection by individual cell culture experts, which hinders the standardization of stem cell cultures and large-scale stem cell manufacturing for applications in regenerative medicine.

Takuya Hirose and Jun'ichi Kotoku contributed equally to this study.

This is an open access article under the terms of the Creative Commons Attribution-NonCommercial-NoDerivs License, which permits use and distribution in any medium, provided the original work is properly cited, the use is non-commercial and no modifications or adaptations are made.

© 2021 The Authors. STEM CELLS published by Wiley Periodicals LLC on behalf of AlphaMed Press.

Human keratinocyte stem cells are among the few adult stem cells that can be extensively and successfully expanded in culture for applications in regenerative medicine.²⁻⁴ Globally, autologous cultured human epidermal keratinocyte stem cells have been used for transplantation in patients with extensive burns for approximately 40 years.⁵⁻⁷ Additionally, these stem cells are used for ex vivo gene therapy of hereditary skin disorders.^{8,9} However, the specific identification of these stem cells in culture is a limiting factor as there are no known reliable cell surface markers.¹⁰ Currently, the human keratinocyte stem cells in culture are unambiguously identified through clonal analysis.^{10,11} The stemness of stem cells can be examined with high accuracy using single-cell clonal analysis. However, the single-cell clonal analysis is time-consuming, expensive, and labor-intensive.

To overcome the limitations associated with clonal analysis¹¹ and xenotransplantation,¹² we had previously reported that the human keratinocyte stem cells can be distinguished from non-stem cells at an early stage in the culture using cell motion analysis.¹³ In this study, we have developed a predictable and reproducible readout to determine the quality of human keratinocyte culture. However, human keratinocytes form densely packed colonies.^{11,14} The motion analysis of individual cells within a colony is performed only through manual cell tracking,^{13,15} which is time-consuming and error-prone. Therefore, there is a need to develop an automated system that provides quantitative information on individual cell behavior within the human keratinocyte colonies during cell manufacturing for regenerative medicine. Previously, we had reported that motion analysis with optical flow can automatically estimate the cell velocity of cultured human keratinocytes and demonstrated a positive correlation between cell velocity and proliferative capacity.^{16,17} However, this method is not an equivalent for cell tracking and does not have the accuracy of manual cell tracking.¹⁷ Hence, there is a need to develop an automated cell tracking method with an accuracy equivalent to manual tracking accuracy for clinical and industrial applications.

The accuracy of disease diagnosis by artificial intelligence (AI) technology using medical images is similar to that by healthcare professionals, which has increased the reliability of AI-based diagnostic assessment.¹⁸⁻²⁰ Deep learning-based AI technology has also been applied to stem cell research and stem cell therapy.²¹⁻²³ Here, we report a deep learning-based automated cell tracking (DeepACT) technology that enables the evaluation of keratinocyte culture quality and the identification of keratinocyte stem cells using quantitative cell motion analysis. DeepACT comprises two main modules: identifying human keratinocytes at single-cell resolution from phase-contrast images of cultures through deep learning and tracking keratinocyte motion in the colony using a state-space model.

2 | MATERIALS AND METHODS

2.1 | Preparation of feeder cells

The 3T3-J2 cells were cultured at 37°C and 10% CO₂ in Dulbecco's modified Eagle's medium (DMEM; Gibco 11995-065) supplemented

Significance statement

The authors developed a novel noninvasive quality control technology for cultured human keratinocyte stem cells constructed by deep learning-based automated cell recognition and Kalman filter algorithm-based tracking. This deep learning-based automated cell tracking (DeepACT) technology rapidly analyzed the motion of keratinocytes and provided the collective motion dynamics in cultured keratinocytes, which enabled the quantitative evaluation of keratinocyte dynamics in response to changes in culture conditions. Furthermore, DeepACT identified human keratinocyte stem cells since the stem cell colonies exhibited a unique motion pattern.

with 10% bovine serum (Sigma-Aldrich C8056). The cells were passaged once a week and maintained up to passage 12. The culture medium was replaced with fresh medium every 3 or 4 days. To prepare the feeder layer, the 3T3-J2 cells were incubated with 4 µg/mL mitomycin C (Kyowa Kirin Co. Ltd.) for 2 hours. The mitomycin C-treated 3T3-J2 cells were washed with phosphate-buffered saline (PBS) twice and trypsinized with 0.05% trypsin-ethylenediaminetetraacetic acid (EDTA) solution (Gibco 25300-054). The trypsinized cells were seeded into the cell culture dishes as feeder cells before the inoculation of keratinocytes.

2.2 | Human keratinocyte culture

Normal human epidermal keratinocytes (KURABO) were isolated from the neonatal skin. The frozen keratinocytes were thawed and cultured at clonal density on a feeder layer of mitomycin C-treated mouse 3T3-J2 fibroblasts. The co-culture was incubated at 37°C and 10% CO₂ in a 3:1 mixture of DMEM (Gibco 11995-065) and Ham's F12 medium (Gibco 11765-054) supplemented with 10% fetal bovine serum (FBS; Biowest 91760-500), 1.8×10^{-4} M adenine hemisulphate salt (Sigma-Aldrich A3159), 5 µg/mL insulin (Sigma-Aldrich I5500), 0.4 µg/mL hydrocortisone (Calbiochem 386698), 10^{-10} M cholera toxin (MP medicals 190329), and 2×10^{-9} M triiodothyronine (T3; Sigma-Aldrich T2752) as described previously.¹³ The keratinocytes between passages 2 and 7 were used for the experiments. The culture medium was replaced with fresh medium every 4 days supplemented with 10 ng/mL recombinant human EGF (Upstate 01-107). Clonal analysis was performed as described previously.^{11,13} Briefly, the human keratinocytes were cultured at clonal density on a feeder layer of mitomycin C-treated 3T3-J2 cells. The isolated colonies were individually trypsinized with 0.05% Trypsin-EDTA solution (Gibco 25300-054) in a cloning ring and seeded into the 6-well cell culture plate. To visualize the keratinocyte colonies, the cultures were

fixed with 3.7% buffered formaldehyde and stained with 1% rhodamine B.

2.3 | Time-lapse imaging

Human epidermal keratinocytes were seeded at clonal density in a 35-mm cell culture dish (Grainer Advanced TC 627965) on a feeder layer of mitomycin C-treated 3T3-J2 cells and cultured at 37°C and 10% CO₂. For time-lapse imaging, the cells were maintained at 37°C and 5% CO₂ in a chamber mounted on a FLUOVIEW FV10i microscope (Olympus). The images were captured at 5-minute intervals mostly for 1–3 hours depending on the experimental conditions.

2.4 | Preparation of cell tracking

Cell tracking was performed in two steps: the cell detection stage and the cell tracking stage using state-space models. At the cell detection stage, the aim was to determine the initial positions of cells and generate observation data. We used a multi-cascading network for cell detection. In this process, the nearest detected cell from the predicted point was assumed as the observation data.

2.4.1 | Processing phase

Initial phase-contrast microscope images (TIFF) with a size of 1024 × 1024 pixels were preprocessed with histogram equalization and converted into 8-bit JPEG images. All the following analyses were performed on these preprocessed images.

2.4.2 | Training data preparation

For cell detection, several training data were required for supervised learning. To prepare these training data, the cells recognized by a biologist through visual analysis were used and each cell region was cropped. The training data comprised positive 18 032 boxes and negative 5628 boxes. An example of some training data is shown in Figure 1A.

2.5 | Deep learning for cell detection

2.5.1 | Cell candidate extraction

To detect the cells, a detection algorithm based on a convolutional network (SSD),²⁴ was used. Before learning, the original training images were augmented as follows: 188 original images were converted to 808 images by performing up, down, left, and right inversions, gamma corrections (0.75, 1.00, 1.25, and 1.50), resolution changes (0.75, 0.85, 1, 1.15, and 1.25). The images were augmented 80 (= 4 × 4 × 5) times to obtain 15 040 images.

2.5.2 | Cell recognition

The extracted candidate cells involved many false-positive results. The correct cells were chosen from these candidates using a cascading network built to classify the candidate boxes accurately. As shown in Figure 1B, the cascading network comprised three deep convolutional networks based on VGG16²⁵ (DCN1, DCN2, DCN3). These deep convolutional networks were trained independently. In the learning step, the data were augmented 72 times using rotation. The images of cells at the mitosis stage were also added to the dictionary. The Adam algorithm minimized the entire network. All networks were implemented with Chainer. A super-computer (Reedbush-L) at the Information Technology Center, University of Tokyo calculated the whole steps for learning.

2.6 | Input data preprocessing

The raw microscope images were preprocessed with histogram equalization before tracking.

2.7 | Cell tracking

In the tracking process, observation data were generated using the following rules. The cell was regarded as an observed cell if the nearest cell was not beyond a distance of 20 pixels from the prediction point, while the other observed data were regarded as missing. The Kalman filter²⁶ filtered all these steps. Supplemental Figure S1A shows an example of the determination of the next cell and missing cells. The red circle at the bottom includes a detected cell, which was regarded as an observed cell. In contrast, when the circle did not include any detected cells, the observation data were regarded as missing data.

2.8 | Calculation of motion index

The motion index was calculated by dividing the average cell velocity in the central region of the colony by that in the marginal region of the colony. The marginal region of each colony comprising 30% of the total colony area is defined as the marginal region. The remaining area (70% of the total colony area) was defined as the central region (Supplemental Figure S1B).

2.9 | Statistics

All statistical analyses were performed using Prism8 (GraphPad Software) and Excel (Microsoft Office 2016). The differences between two groups were analyzed using the unpaired two-tailed Mann-Whitney *U*-test and chi-squared test. The differences between multiple groups were analyzed using one-way analysis of variance (ANOVA), followed by Tukey's post hoc test. The differences were considered statistically significant when the *P*-value was less .05.

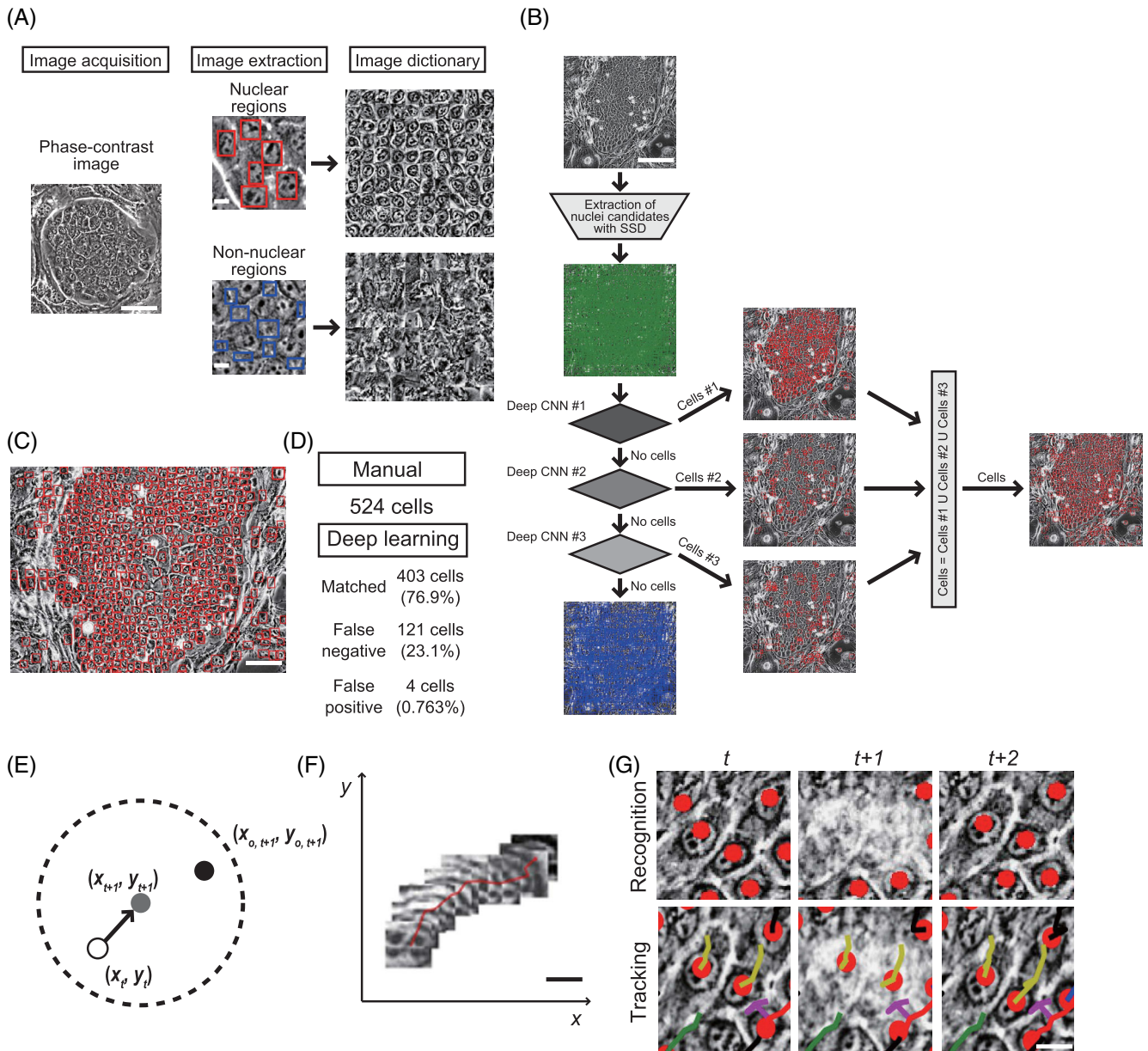


FIGURE 1 Development of deep learning-based object tracking model for automated cell tracking in human keratinocyte colonies.

A, Preparation of image dictionaries for deep learning using the phase-contrast images of cultured human keratinocytes. Scale bar = 100 μm for left panel, and 10 μm for middle panel. B, Single shot multi-box detector (SSD)-based deep learning model for nuclear recognition. Scale bar = 200 μm . C, Automated nuclear recognition by the trained SSD-based deep learning model. The recognized nuclei are indicated in red boxes. Scale bar = 100 μm . D, Accuracy of automated nuclear recognition. Five hundred and twenty-four keratinocytes were extracted from this phase-contrast image of the keratinocyte colony by visual recognition. About 80% of keratinocytes are also automatically recognized by the trained SSD deep learning model. The 3T3-J2 cells were excluded from the analysis. E, Moving object tracking using the Kalman filter algorithm. F, Tracking of a nucleus automatically recognized from the time-series phase-contrast images of human keratinocytes. Scale bar = 10 μm . G, Successive tracking of nuclei in the culture containing cellular debris. The Kalman filter algorithm skips the image if the nucleus is not recognized within the predicted region and performs tracking with the next time-series image. Scale bar = 10 μm

3 | RESULTS

3.1 | Automated recognition of keratinocyte nuclei through deep learning

We captured a large number of images of nuclear and non-nuclear regions in the cultured human keratinocytes, which were

used to generate an image dictionary for training the deep learning model. In total, 18 031 nuclear and 5632 non-nuclear images were identified through manual analysis (Figure 1A). Next, the images were automatically processed through image inversion and gamma correction to obtain a keratinocyte image dictionary comprising a large amount of processed data (see details in Materials and Methods).

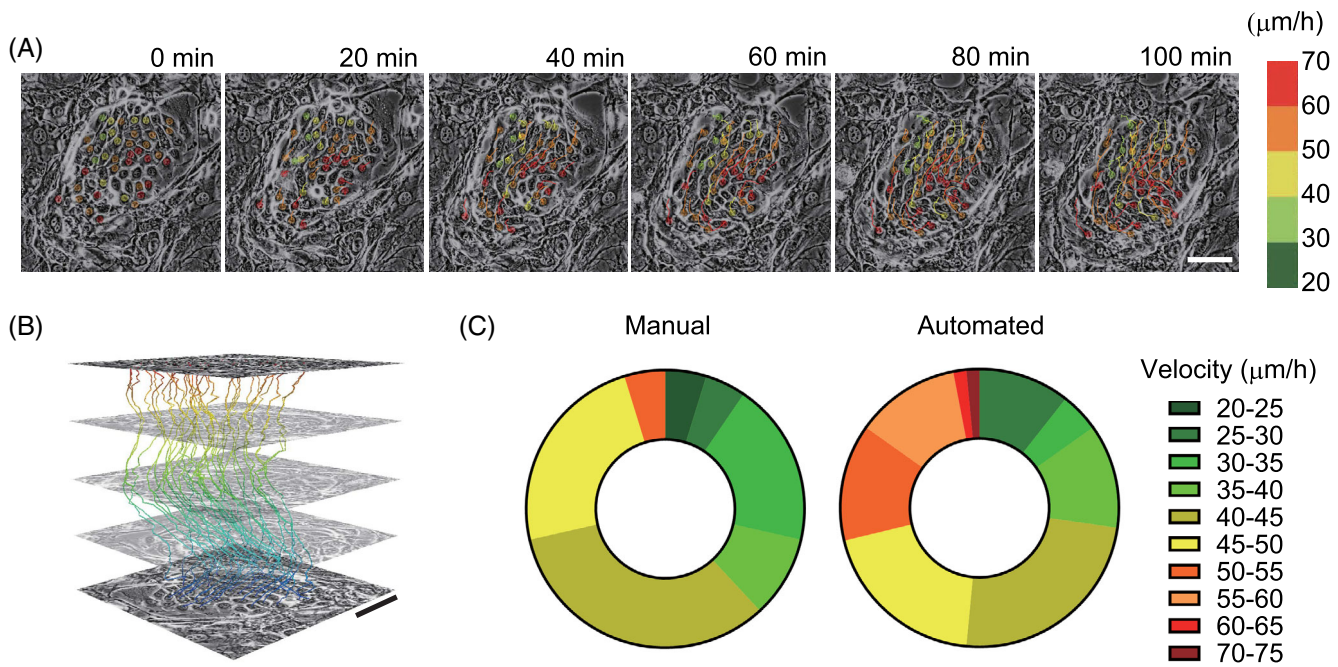


FIGURE 2 Automated cell tracking in human keratinocyte colonies. A, Automated cell tracking by a combination of deep learning-based nuclear recognition and Kalman filter algorithm-based tracking (see also Supplemental Movie S1). The circles and lines show the nuclei and their trajectories, respectively. The color indicates the magnitude of cell velocity, as shown on the right. Scale bar = 100 μm . B, The 3D image indicates the changes in nuclear positions along with the time as lines for 12 hours. Scale bar = 100 μm . C, Comparison of manual and automated tracking. The velocity distributions were analyzed by manual and automated tracking. The color indicates the magnitude of cell velocity as shown on the right

This dictionary was used to train a single shot multi-box detector (SSD)-based deep learning model. Several neural networks were also organized for automated nuclear recognition in the cultured human keratinocytes. In the automated system, after a keratinocyte colony image is fed to the machine, the SSD lines up the candidate region and each neural network identifies the nucleus of individual keratinocytes based on different criteria. The output is a combination of the results from each neural network (Figure 1B).

This system could automatically identify the nuclei of cultured human keratinocytes (Figure 1C). To evaluate the accuracy of automated nuclear recognition, the output images processed by the trained deep learning model were compared with those processed by manual analysis. Manual analysis revealed that the original image contained 524 keratinocyte nuclei (Figure 1D); whereas the deep learning model-based image processing revealed that the image contained 407 keratinocyte nuclei. Of these 407 nuclei, 403 matched with the nuclei detected using manual analysis and only 4 nuclei were detected as false positives (Figure 1D). However, 121 keratinocyte nuclei identified in the manual analysis were not identified in the automated analysis (false-negative). Thus, the SSD-based deep learning model could detect approximately 76.9% of the keratinocyte nuclei with high accuracy.

3.2 | Tracking of nuclei using the Kalman filter

Individual identical nuclei can be tracked by analyzing the nuclei in time-series images. We developed a novel cell tracking system

adapted to the cell cultures. To track the keratinocyte nuclei identified by the deep learning-based automated system, we applied a framework of state-space models, especially an algorithm called Kalman filter. This algorithm can predict the position of a moving object based on previous observations and compare the predicted position and measured position at a certain time point (Figure 1E and see details in Materials and Methods and Supplemental Figure S1A). The Kalman filter algorithm successfully tracked an automatically recognized nucleus in the colony (Figure 1F). Furthermore, if a nucleus is not detected within the predicted area, this image was skipped and the next time-series image was used for tracking. The presence of a high amount of cell debris in the cell cultures, especially those derived from tissues, disrupts cell tracking. However, the automated system could track the cells even in the presence of cellular debris (Figure 1G). This indicated that the tracking system can be adapted to cell cultures used for cell therapy.

3.3 | Evaluation of automated cell tracking

The deep learning-based automated nuclear recognition system and Kalman filter algorithm was used to analyze the time-series phase-contrast images of a human keratinocyte colony. The system successfully recognized and tracked most cells in the colony and automatically determined the velocity of individual cells in the colony every hour (Figure 2A and Supplemental Movie S1). Additionally, the system determined the pattern of cell locomotion (Figure 2B). The nuclear

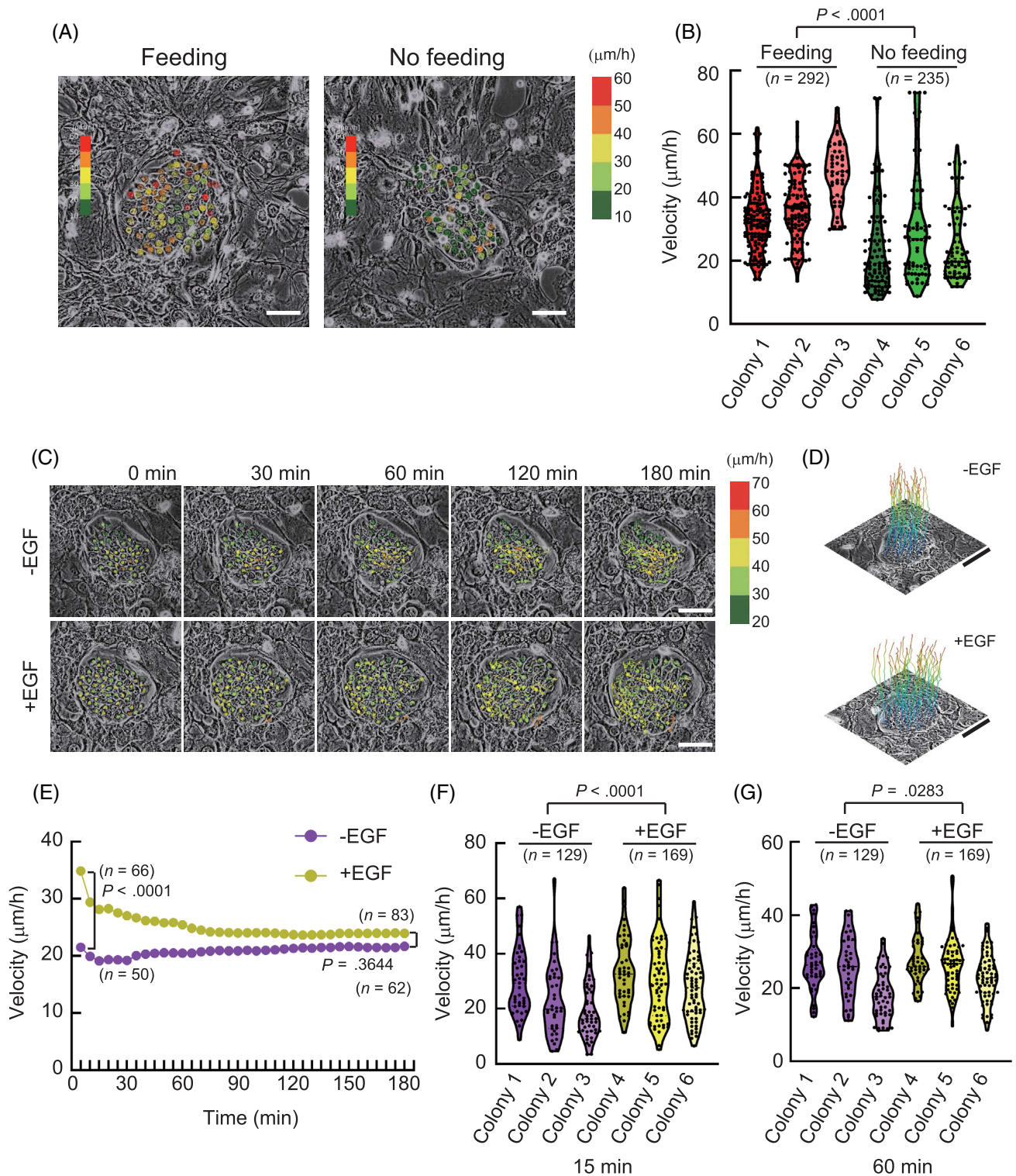


FIGURE 3 Quantitative evaluation of keratinocyte behavior in response to changes in culture conditions. A, Automated cell tracking in the human keratinocyte cultures with and without feeding (see also Supplemental Movies S2 and S3). The velocity of the individual cells is indicated with the color shown on the right. Scale bar = 100 μm . B, Violin plots of cell velocity measured by automated cell tracking of keratinocyte colonies with and without feeding. Three colonies were analyzed under each condition. C, Automated cell tracking of human keratinocyte cultures with and without epidermal growth factor (EGF) (see also Supplemental Movies S4 and S5). Tracking was started approximately 30 minutes after the addition of 10 $\mu\text{g/mL}$ EGF. The velocity of the individual cells is indicated with the color shown on the right. Bars, 200 μm . D, The 3D image indicates the changes in nuclear positions along with the time as lines for 180 minutes. Bars, 200 μm . E, The changes in the average cell velocity with and without EGF treatment in the same keratinocyte colony. Tracking was started approximately 30 minutes after EGF addition. F and G, Violin plots of cell velocity measured by automated cell tracking of keratinocyte colonies with and without EGF treatment. Data obtained from 15 (F) and 60 (G) min after tracking are shown. Three colonies were analyzed under each condition. P -values for cell velocity under each condition were calculated using the Mann-Whitney U -test

detection accuracies of automated nuclear tracking and manual nuclear tracking were comparatively analyzed. The velocity distributions of cells in the colony analyzed using manual and automated cell tracking were similar but not identical (Figure 2C). In particular, the automated tracking revealed higher population of fast-moving cells than the manual tracking. This is because the automated system recognizes and tracks two different cells as identical cells. However, the combination of deep learning-based nuclear recognition and Kalman filter algorithm-based object correctly tracked most cells in the colony.

3.4 | Quantitative evaluation of the collective dynamics of keratinocytes in response to changes in culture conditions

Noninvasive real-time monitoring of cell cultures is required for quality and production control of cultured cells. The application of DeepACT for the quality and production control of human keratinocyte cultures was evaluated. In this study, the cultures were fed at day 4 post-inoculation. The locomotion of individual keratinocytes in the colony was observed on day 5 post-inoculation (Supplemental Movie S2). The DeepACT system quantified the cell locomotion in the colony by analyzing the time-series phase-contrast images (Figure 3A and B). When the culture was not fed as per schedule, the DeepACT analysis revealed significantly decreased keratinocyte locomotion (Supplemental Movie S3 and Figure 3A,B). Therefore, cell locomotion velocity can be used as a noninvasive parameter for determining the optimal cell culture conditions.

The human keratinocyte culture must be supplemented with epidermal growth factor (EGF) during mass expansion.²⁷⁻²⁹ The addition of EGF and subsequent activation of EGF receptor (EGFR) induces the outward migration of keratinocytes in the colony.^{14,28} The DeepACT system could detect the EGF-induced change in cell migration pattern (Supplemental Movies S4 and S5, and Figure 3C,D). Furthermore, quantitative cell motion analysis using the DeepACT system revealed that the activation of EGFR accelerates the velocity of individual cells in the colony within a short duration (Figure 3E-G). These results indicate that EGFR activation in keratinocytes can be noninvasively detected based on the change in cell locomotion pattern and velocity, which can be monitored through automated cell tracking. Thus, the DeepACT system can be applied to monitor the cell culture conditions for quality and production control of cultured human keratinocytes.

3.5 | Automated cell tracking identifies human epidermal keratinocyte stem cell colonies

Previously, we had demonstrated that the average velocity of keratinocyte locomotion in the colony is positively correlated with the long-term proliferative capacity of keratinocytes.^{13,17} The DeepACT system was used to identify the human keratinocyte stem cell

colonies. Time-lapse imaging of keratinocyte colonies was performed at day 6 post-inoculation for 1 hour. Each colony was subcloned into a new cell culture plate (Figure 4A). To evaluate the long-term proliferative capacity of individual clones, each clone was categorized into three clonal types according to the guidelines of Barrandon and Green 1987,¹¹ which are the gold standard for the assessment of long-term proliferative capacity of human keratinocytes. Holoclones can maintain their growth potential and form progressively growing colonies after passage. Paraclones lose their proliferative capacity and generate only differentiated terminal colonies after the passage. Meroclones exhibit an intermediate phenotype and generate both growing and terminal colonies. There was no correlation between the areas of each colony before cloning and its clonal type (Figure 4B). The clonal types of individual human keratinocyte colonies were correlated with the total area of keratinocyte colonies in the replated cultures after subcloning (Figure 4C).

The DeepACT system could determine the velocity of cells in the colony. There was no correlation between the average velocity of cell locomotion and long-term proliferative capacity (Supplemental Figure S2A,B). The DeepACT system sometimes did not recognize keratinocytes located in the central region of the colony. This indicates that the calculated average velocity was majorly based on the velocity of cells located in the marginal region of the colony. In a previous study, we calculated the average velocity of cells using the locomotion velocity of randomly selected cells located at both the central and the marginal regions of the colony.¹³ Here, we analyzed the velocity data using a function that calculates the motion index, a value indicating the motion dynamics of individual keratinocytes in the colony. Motion indices are derived from the ratio of the average velocity of cells at the central region to that at the marginal regions of the colony (see details in Materials and Methods and Supplemental Figure S1B). The motion index of less than 1.0 indicates that the cells located in the marginal region of the colony move faster than those in the central region. Conversely, a motion index of more than 1.0 indicates that the cells located in the central region move faster than those in the marginal region. The clonal analysis revealed that the paraclone-derived colonies exhibited a low motion index. In contrast, the holoclone-derived colonies exhibited high motion index (Figure 4D). When the colonies with the highest motion index (>1.0) were selected, the probability of obtaining holoclone-derived colonies significantly increased (odds ratio = 4.5, $P = .04181$, by chi-square test) (Figure 4E). These results indicate that cell motion analysis using the DeepACT system can identify human keratinocyte stem cell colonies without cell culture labeling and that this system can be applied for quality control of keratinocyte cultures used in cell therapy.

4 | DISCUSSION

Deep learning-based image recognition has advanced the field of biomedical science and has been applied for AI-based disease diagnosis. In this study, we demonstrated that the quality of human keratinocyte

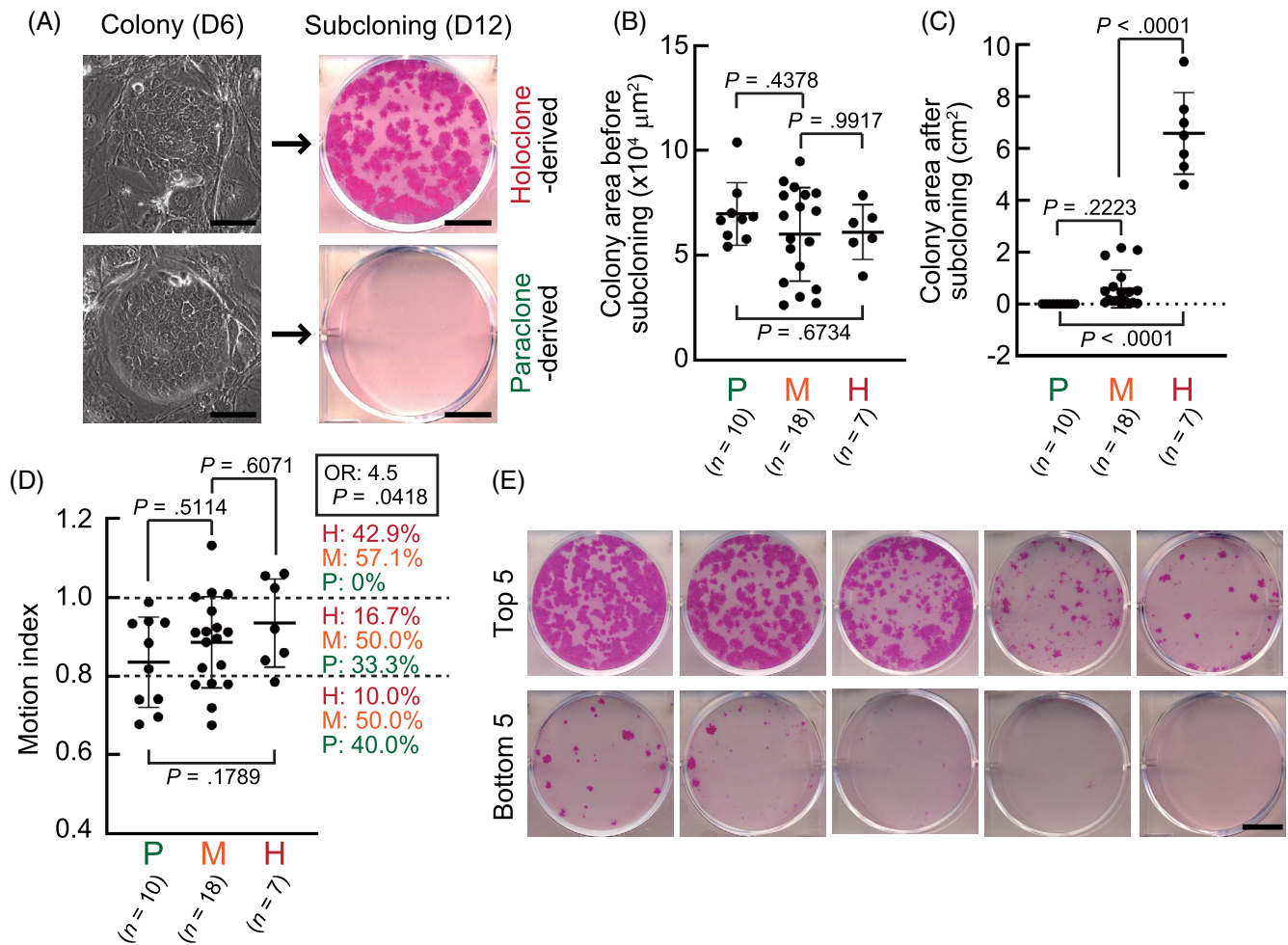


FIGURE 4 Human keratinocyte stem cell colonies were identified by automated cell tracking. A, Clonal analysis of human keratinocytes. Time-lapse imaging of a progressively growing colony was performed. The colony was subcultured into a new cell culture plate for evaluation of clonal types. Scale bar = 100 μm in left panel and 10 mm in right panel. B, The colony area of growing colonies before subcloning was not correlated with the following three clonal types: paraclones (P), meroclones (M), and holoclones (H). C, The colony area of subcultured growing colonies was correlated with their clonal types. D, The distribution of the motion index of keratinocyte colonies derived from three clonal types. Motion indices were calculated with automated cell tracking as shown in the Materials and Methods and Supplemental Figure S1B. In the right panel, the percentages of each clonal type in three motion index classes ($\text{MI} > 1.0$, $1.0 \geq \text{MI} > 0.8$, $\text{MI} \leq 0.8$) are presented. The odds ratio and its P -value calculated using the chi-squared test (probability of holoclone-derived colonies in the colonies with $\text{MI} > 1.0$ against the colonies with $\text{MI} \leq 1.0$) are described in the box. E, Images of cell cultures after subcloning of keratinocyte colonies with various motion indices. The subcultures of five colonies from the top (upper) and bottom (lower) are shown. Scale bar = 10 mm. P -values, except for the right panel in D, were calculated using one-way analysis of variance (ANOVA), followed by Tukey's multiple comparison test

stem cells could be predicted by analyzing the collective motion dynamics with a combination of deep learning-based image recognition and Kalman filter algorithm-based moving object tracking. The success of cell therapy for severe burns⁶ and corneal blindness³⁰ is dependent on optimal ex vivo maintenance and expansion of keratinocyte stem cells. During culture, the keratinocyte stem cells (holoclones) are transformed into meroclones and paraclones, which exhibit restricted growth potentials under suboptimal culture conditions.^{10,14} The efficiency of transplantation decreases as the number of holoclones decreases in the culture due to clonal conversion even if the generated epithelial sheets are engrafted successfully.³¹⁻³³ The DeepACT system can directly estimate the number of colonies derived from holoclones on cell culture dishes and flasks, which enables the

selection of cultures suitable for transplantation before preparing the confluent keratinocyte sheets. Efficient isolation of holoclone-derived colonies, which have applications in gene therapy, has been achieved using a clonal population of genetically modified keratinocytes.³⁴

Previously, we had demonstrated that the human keratinocyte stem cell colonies exhibit a locomotive phenotype.^{13,17} However, the cell motion analysis using the DeepACT system revealed that the average velocity of stem cells was not positively correlated with the proliferative potential of keratinocyte colonies. This was because the automated system did not recognize the nucleus of keratinocytes located at the central region of the colony. Furthermore, this study demonstrated that the measured cell velocity varies depending on the cell culture conditions. Thus, the absolute value of cell velocity may

not be a suitable indicator of “good” keratinocyte cultures suitable for transplantation. In contrast, the motion index is a relative value and can be used as a comparative parameter among cell cultures. Motion index of more than 1.0 indicates the long-term proliferative capacity of keratinocyte, which suggests that the cells located in the central region of the holoclone-derived colony move faster than those located in the marginal region. This has also been predicted in our previous observation and simulation experiments.¹³ These results indicate that the homogeneity of cell locomotion velocities is one of the characteristics of holoclone-derived colonies and that the motion index is a predictable and reproducible readout of growth potentials of human keratinocyte colonies. Hence, the colonies exhibiting motion index >1.0 during the production of keratinocyte sheets might be an indicator of “good” cultures, which can be used for successful transplantation.

The cascading cell detection model, which was trained using the phase-contrast images of cultured human epidermal keratinocytes, achieved automated nuclear recognition in the keratinocytes. This system can also be directly applied to human keratinocyte cultures used for regenerative medicine of other stratified squamous epithelia, including corneal, oral mucosal, and esophageal epithelia.^{30,35-37} Furthermore, the trained SSD model can be easily utilized for automated nuclear recognition of other types of cells with “transfer learning.” This system can also be applied to other types of cell cultures with a smaller number of image data. Collective cell motion is observed in various cells,³⁸ including neural progenitor cells,³⁹ and human keratinocytes in epidermal⁴⁰ and corneal sheets.⁴¹ Furthermore, cell motility is associated with the state of human embryonic stem cells (hESCs)⁴² and human induced pluripotent stem cells (hiPSCs),⁴³ which strongly suggests that automated cell motion analysis can be also applied to quality control of human pluripotent stem cell cultures. Thus, the DeepACT technology can be widely used for stem cell research and cell manufacturing for regenerative medicine.

To further advance stem cell-based regenerative medicine, the cell cultures should be automatically processed, which enables stable supply of high-quality cells and decreased cell production cost for industrial cell manufacturing. Recently, several automated cell culture systems using human stem cells have been developed for applications in regenerative medicine.⁴⁴⁻⁴⁸ However, these systems do not incorporate in situ and noninvasive quality control of cell production. DeepACT can be used for reliable real-time monitoring of cell cultures and for selecting cell cultures suitable for transplantation. Cell motion analysis-based stem cell quality control can be easily implemented in automated cell culture devices, which provide an intelligent cell culture system for fabricating high-quality stem cell-based products with increased sterility and safety.

5 | CONCLUSION

We developed the DeepACT technology that successfully tracks the individual cells within the densely packed human epidermal keratinocyte colonies in the phase-contrast images of the culture. Our data demonstrate that automated cell motion analysis enables the

quantitative evaluation of keratinocyte dynamics in response to changes in culture conditions and label-free identification of human keratinocyte stem cells. This technology can be widely applied to stem cell cultures used in regenerative medicine.

ACKNOWLEDGMENTS

We thank Prof. H. Toki (Osaka University) for his continuous encouragement and Japan Tissue Engineering Co., Ltd. (Gamagori, Japan) for providing the 3T3-J2 cells. This work was supported by Japan Society for the Promotion of Science KAKENHI Grant (17K102319), by a Grand-in-Aid for Scientific Research on Innovative Area “Singularity Biology (No. 8007)” (19H05418) of The Ministry of Education, Culture, Sports, Science, and Technology, Japan, and by the Okawa Foundation (19-08) to D.N.

CONFLICT OF INTEREST

The authors declared no potential conflicts of interest.

AUTHOR CONTRIBUTIONS

T.H.: system development, data analysis and interpretation; J.K.: conception and design, system development, manuscript writing; F.T.: cell cultures, collection of data, data analysis and interpretation; E.K.N.: data analysis and interpretation, supervision; D.N.: conception and design, data analysis and interpretation, manuscript writing.

DATA AVAILABILITY STATEMENT

The authors declare that all data supporting the findings of this study are available within the manuscript or are available from the corresponding authors upon request.

ORCID

Daisuke Nanba  <https://orcid.org/0000-0002-9765-9113>

REFERENCES

- De Luca M, Aiuti A, Cossu G, et al. Advances in stem cell research and therapeutic development. *Nat Cell Biol.* 2019;21:801-811.
- Green H. The birth of therapy with cultured cells. *Bioessays.* 2008;30:897-903.
- Hynds RE, Bonfanti P, Janes SM. Regenerating human epithelia with cultured stem cells: feeder cells, organoids and beyond. *EMBO Mol Med.* 2018;10:139-150.
- Nanba D. Human keratinocyte stem cells: from cell biology to cell therapy. *J Dermatol Sci.* 2019;96:66-72.
- O'Connor NEMJ, Banks-Schlegel S, Kehinde O, Green H. Grafting of burns with cultured epithelium prepared from autologous epidermal cells. *Lancet.* 1981;1:75-78.
- Gallico GG 3rd, O'Connor NE, Compton CC, et al. Permanent coverage of large burn wounds with autologous cultured human epithelium. *N Engl J Med.* 1984;311:448-451.
- Pellegrini G, De Luca M. Living with keratinocytes. *Stem Cell Rep.* 2018;11:1026-1033.
- Mavilio F, Pellegrini G, Ferrari S, et al. Correction of junctional epidermolysis bullosa by transplantation of genetically modified epidermal stem cells. *Nat Med.* 2006;12:1397-1402.
- Hirsch T, Rothoefel T, Teig N, et al. Regeneration of the entire human epidermis using transgenic stem cells. *Nature.* 2017;551:327-332.

10. Barrandon Y, Grasset N, Zaffalon A, et al. Capturing epidermal stemness for regenerative medicine. *Semin Cell Dev Biol.* 2012;23:937-944.
11. Barrandon Y, Green H. Three clonal types of keratinocyte with different capacities for multiplication. *Proc Natl Acad Sci USA.* 1987;84:2302-2306.
12. Barrandon Y, Li V, Green H. New techniques for the grafting of cultured human epidermal cells onto athymic animals. *J Invest Dermatol.* 1988;91:315-318.
13. Nanba D, Toki F, Tate S, et al. Cell motion predicts human epidermal stemness. *J Cell Biol.* 2015;209:305-315.
14. Nanba D, Toki F, Matsushita N, Matsushita S, Higashiyama S, Barrandon Y. Actin filament dynamics impacts keratinocyte stem cell maintenance. *EMBO Mol Med.* 2013;5:640-653.
15. Roshan A, Murai K, Fowler J, Simons BD, Nikolaidou-Neokosmidou V, Jones PH. Human keratinocytes have two interconvertible modes of proliferation. *Nat Cell Biol.* 2016;18:145-156.
16. Hoshikawa E, Sato T, Kimori Y, et al. Noninvasive measurement of cell/colony motion using image analysis methods to evaluate the proliferative capacity of oral keratinocytes as a tool for quality control in regenerative medicine. *J Tissue Eng.* 2019;10:2041731419881528.
17. Kinoshita K, Munesue T, Toki F, et al. Automated collective motion analysis validates human keratinocyte stem cell cultures. *Sci Rep.* 2019;9:18725.
18. Esteva A, Kuprel B, Novoa RA, et al. Dermatologist-level classification of skin cancer with deep neural networks. *Nature.* 2017;542:115-118.
19. Ehteshami Bejnordi B, Veta M, Johannes van Diest P, et al. Diagnostic assessment of deep learning algorithms for detection of lymph node metastases in women with breast cancer. *JAMA.* 2017;318:2199-2210.
20. Kermany DS, Goldbaum M, Cai W, et al. Identifying medical diagnoses and treatable diseases by image-based deep learning. *Cell.* 2018;172:1122-1131.e1129.
21. Buggenthin F, Buettner F, Hoppe PS, et al. Prospective identification of hematopoietic lineage choice by deep learning. *Nat Methods.* 2017;14:403-406.
22. Kusumoto D, Lachmann M, Kunihiro T, et al. Automated deep learning-based system to identify endothelial cells derived from induced pluripotent stem cells. *Stem Cell Rep.* 2018;10:1687-1695.
23. Waisman A, La Greca A, Mobbs AM, et al. Deep learning neural networks highly predict very early onset of pluripotent stem cell differentiation. *Stem Cell Rep.* 2019;12:845-859.
24. Liu W, Anguelov D, Erhan D, et al. ISSD: Single Shot MultiBox Detector. In: Leibe B, Matas J, Sebe N, Welling M, eds. *Computer Vision – ECCV 2016. ECCV 2016. Lecture Notes in Computer Science.* Vol. 9905. Cham: Springer; 2016. https://doi.org/10.1007/978-3-319-46448-0_2
25. Simonyan K, Zisserman A. Very Deep Convolutional Networks for Large-Scale Image Recognition. arXiv preprint arXiv:1409.1556; 2014.
26. Kalman RE. A new approach to linear filtering and prediction problems. *J Basic Eng.* 1960;82:35-45.
27. Rheinwald JG, Green H. Epidermal growth factor and the multiplication of cultured human epidermal keratinocytes. *Nature.* 1977;265:421-424.
28. Barrandon Y, Green H. Cell migration is essential for sustained growth of keratinocyte colonies: the roles of transforming growth factor- α and epidermal growth factor. *Cell.* 1987;50:1131-1137.
29. Nanba D, Toki F, Barrandon Y, Higashiyama S. Recent advances in the epidermal growth factor receptor/ligand system biology on skin homeostasis and keratinocyte stem cell regulation. *J Dermatol Sci.* 2013;72:81-86.
30. Pellegrini G, Traverso CE, Franzi AT, Zingirian M, Cancedda R, de Luca M. Long-term restoration of damaged corneal surfaces with autologous cultivated corneal epithelium. *Lancet.* 1997;349:990-993.
31. Dunnwald M, Tomanek-Chalkley A, Alexandrunas D, Fishbaugh J, Bickenbach JR. Isolating a pure population of epidermal stem cells for use in tissue engineering. *Exp Dermatol.* 2001;10:45-54.
32. Rama P, Matuska S, Paganoni G, Spinelli A, de Luca M, Pellegrini G. Limbal stem-cell therapy and long-term corneal regeneration. *N Engl J Med.* 2010;363:147-155.
33. Pellegrini G, Rama P, Matuska S, et al. Biological parameters determining the clinical outcome of autologous cultures of limbal stem cells. *Regen Med.* 2013;8:553-567.
34. Droz-Georget Lathion S, Rochat A, Knott G, et al. A single epidermal stem cell strategy for safe ex vivo gene therapy. *EMBO Mol Med.* 2015;7:380-393.
35. Nishida K, Yamato M, Hayashida Y, et al. Corneal reconstruction with tissue-engineered cell sheets composed of autologous oral mucosal epithelium. *N Engl J Med.* 2004;351:1187-1196.
36. Izumi K, Feinberg SE, Iida A, Yoshizawa M. Intraoral grafting of an ex vivo produced oral mucosa equivalent: a preliminary report. *Int J Oral Maxillofac Surg.* 2003;32:188-197.
37. Ohki T, Yamato M, Ota M, et al. Prevention of esophageal stricture after endoscopic submucosal dissection using tissue-engineered cell sheets. *Gastroenterology.* 2012;143:582-588.e582.
38. Rorth P. Collective cell migration. *Annu Rev Cell Dev Biol.* 2009;25:407-429.
39. Kawaguchi K, Kageyama R, Sano M. Topological defects control collective dynamics in neural progenitor cell cultures. *Nature.* 2017;545:327-331.
40. Lang E, Polec A, Lang A, et al. Coordinated collective migration and asymmetric cell division in confluent human keratinocytes without wounding. *Nat Commun.* 2018;9:3665.
41. Baba K, Sasaki K, Morita M, et al. Cell jamming, stratification and p63 expression in cultivated human corneal epithelial cell sheets. *Sci Rep.* 2020;10:9282.
42. Barbaric I, Biga V, Gokhale PJ, et al. Time-lapse analysis of human embryonic stem cells reveals multiple bottlenecks restricting colony formation and their relief upon culture adaptation. *Stem Cell Rep.* 2014;3:142-155.
43. Shuzui E, Kim MH, Kino-Oka M. Anomalous cell migration triggers a switch to deviation from the undifferentiated state in colonies of human induced pluripotent stems on feeder layers. *J Biosci Bioeng.* 2019;127:246-255.
44. Kami D, Watakabe K, Yamazaki-Inoue M, et al. Large-scale cell production of stem cells for clinical application using the automated cell processing machine. *BMC Biotechnol.* 2013;13:102.
45. Soares FA, Chandra A, Thomas RJ, et al. Investigating the feasibility of scale up and automation of human induced pluripotent stem cells cultured in aggregates in feeder free conditions. *J Biotechnol.* 2014;173:53-58.
46. Konagaya S, Ando T, Yamauchi T, Suemori H, Iwata H. Long-term maintenance of human induced pluripotent stem cells by automated cell culture system. *Sci Rep.* 2015;5:16647.
47. Daniszewski M, Crombie DE, Henderson R, et al. Automated cell culture systems and their applications to human pluripotent stem cell studies. *SLAS Technol.* 2018;23:315-325.
48. Matsumoto E, Koide N, Hanzawa H, et al. Fabricating retinal pigment epithelial cell sheets derived from human induced pluripotent stem cells in an automated closed culture system for regenerative medicine. *PLoS One.* 2019;14:e0212369.

SUPPORTING INFORMATION

Additional supporting information may be found online in the Supporting Information section at the end of this article.

How to cite this article: Hirose T, Kotoku J, Toki F, Nishimura EK, Nanba D. Label-free quality control and identification of human keratinocyte stem cells by deep learning-based automated cell tracking. *Stem Cells.* 2021;1-10. <https://doi.org/10.1002/stem.3371>